

## Mono- and Terfluorene Oligomers as Versatile Sensitizers for the Luminescent $\text{Eu}^{3+}$ Cation

D. Samuel Oxley, Robert W. Walters, James E. Copenhafer, Tara Y. Meyer,\* Stéphane Petoud,\* and Harry M. Edenborn\*

National Energy Technology Laboratory, U.S. Department of Energy, Pittsburgh, Pennsylvania 15236, and Department of Chemistry, The University of Pittsburgh, Pittsburgh, Pennsylvania 15260

Received February 4, 2009

We present the design, synthesis, and physical and photophysical characterization of  $\text{Eu}^{3+}$  and  $\text{Gd}^{3+}$  complexes formed with two ligands bearing either one or three fluorene sensitizer units. As a novel sensitizing approach, the oligomer length is used to control the energies of the triplet states of the sensitizer and to mediate the sensitizer to lanthanide energy transfer.

The unique electronic structures of lanthanide cations make them highly desirable for a broad range of bioanalytical and technological applications.<sup>1–5</sup> However, since f–f transitions are forbidden,<sup>1</sup> free luminescent lanthanide cations have extremely low extinction coefficients and direct lanthanide excitation results only in modest luminescence intensities. Fortunately, it is possible to increase the signal detection efficiency using the “antenna effect”, which enhances the luminescence intensity by exploiting a suitable sensitizer moiety.<sup>6</sup>

The synthesis of ligands incorporating fluorene oligomer building blocks is a new approach to the generation of luminescent lanthanide complexes with controlled photophysical properties. The triplet-state energies of the different oligomer sensitizers depend on the number of oligomers present in each building block, and the energy of the triplet state is one of the main parameters controlling the intramolecular energy transfer. Klaerner and Miller have demonstrated that the absorption energies of discrete oligomers of fluorene are related to the energies of singlet states of these moieties; red shifts are observed as the length of the oligomer is increased.<sup>7</sup> An additional requirement for the formation of lanthanide complexes with useful emission intensities is the

protection of the luminescent cations against nonradiative deactivation.<sup>8</sup> Both requirements need to be taken into account in the design of the system.

We present here the results of our novel lanthanide coordination and sensitization strategy. The ligands consist of three independent components: a sensitizing unit (fluorene monomer or oligomer), a linker or spacer group, and a chelating unit for lanthanide coordination (Figure 1).

This linker has a well-defined length that is one of the parameters controlling the sensitizer-to-lanthanide energy transfer. The chelating group, derived from diethylenetriaminepentaacetic acid (DTPA), provides strong coordination for the lanthanide (preventing the dissociation of the complex at low concentration).<sup>9</sup> Each of these three components can be tailored to allow for the tuning of the global properties of the resulting luminescent complexes. This approach avoids the reengineering and study of a completely new lanthanide complex system each time a modification is required.

To the best of our knowledge, the use of fluorene oligomers for the sensitization of luminescent lanthanide cations has only been reported in a unique example by Ling et al.<sup>10</sup> The design of their ligand-sensitizer system is fundamentally different from ours in that the fluorene moieties in their alternating copolymer each bear a single bidentate ligand. Coordination of the lanthanide is achieved by the assembly of three units around  $\text{Eu}^{3+}$  rather than the coordination of  $\text{Eu}^{3+}$  by a preorganized polydentate ligand, as is reported herein. Moreover, their system does not exploit the conjugation of a monodisperse oligofluorene for the tuning of system properties.

The complexes were prepared by reacting diamines **1** and **2** with a stoichiometric amount of DTPA anhydride in dimethyl sulfoxide (DMSO) with triethylamine or 1,8-diazabicyclo[5.4.0]undec-7-ene as a base. The <sup>1</sup>H NMR spectrum of the isolated products was consistent with the formation of fluorene–DTPA conjugates; elemental analysis confirmed the

\*To whom correspondence should be addressed. E-mail: tmeyer@pitt.edu (T.Y.M.), spetoud@pitt.edu (S.P.), Harry.Edenborn@netl.doe.gov (H.M.E.).

(1) Bünzli, J.-C. G.; Piguet, C. *Chem. Soc. Rev.* **2005**, 34, 1048–1077.  
(2) Hemmila, I.; Mukkala, V. M. *Crit. Rev. Clin. Lab. Sci.* **2001**, 38, 441–519.  
(3) Leif, R. C.; Vallarino, L. M.; Becker, M. C.; Yang, S. *Cytometry A* **2006**, 767–778.  
(4) Mathis, G. J. *Biomolecul. Screen.* **1999**, 4, 309–313.  
(5) Parker, D.; Dickins, R. S.; Puschmann, H.; Crossland, C.; Howard, J. A. K. *Chem. Rev.* **2002**, 102, 1977–2010.  
(6) Weissman, S. I. *J. Chem. Phys.* **1942**, 10, 214–17.  
(7) Klaerner, G.; Miller, R. D. *Macromolecules* **1998**, 31, 2007–2009.

(8) Beeby, A.; Clarkson, I. M.; Dickins, R. S.; Faulkner, S.; Parker, D.; Royle, L.; de Sousa, A. S.; Williams, J. A. G.; Woods, M. *J. Chem. Soc., Perkin Trans. 2* **1999**, 493–504.

(9) Selvin, P. R.; Jancarik, J.; Li, M.; Hung, L.-W. *Inorg. Chem.* **1996**, 35, 700–5.

(10) Ling, Q. D.; Kang, E. T.; Neoh, K. G.; Huang, W. *Macromolecules* **2003**, 36, 6995–7003.

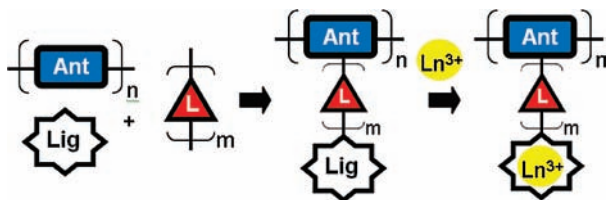


**Figure 1.** Schematic cartoon representing the conceptual design of the coordination and sensitization of lanthanide cations by the assembly of several building blocks that can be replaced without reengineering of the whole molecule (Ant = antenna; Lig = ligand; L = linker;  $\text{Ln}^{3+}$  = lanthanide cation).

**Table 1.** Summary of the Energies of Singlet and Triplet States of the Mono- and Terfluorene Ligands Coordinated to  $\text{Gd}^{3+}$

| complex              | $E(^1\pi\pi^*)$ ( $\text{cm}^{-1}$ ) <sup>a</sup> | $E(^3\pi\pi^*)$ ( $\text{cm}^{-1}$ ) <sup>b</sup> |
|----------------------|---|---|
| F1- $\text{Gd}^{3+}$ | 27 855  | 22 624  |
| F3- $\text{Gd}^{3+}$ | 25 000, 23 809                                    | 18 018  |

<sup>a</sup> Estimated from the apparent maximum (maxima) of the electronic envelope(s) of the fluorescence spectrum (spectra) at 295 K,  $10^{-6}$  M DMSO. <sup>b</sup> Measured as the apparent maximum of the electronic envelope of the phosphorescence spectrum at 77 K,  $10^{-3}$  M frozen DMSO solution, time-resolved measurement.

1:1 ratio. The extremely poor solubility of the conjugate combined with mass spectrometry showing high molecular weight fragments made it clear that the samples consisted of a mixture of monomeric (nonlinked) and oligomeric (linked) species. The linked moieties were present independently of the reaction conditions, and it proved impossible to separate the linked and nonlinked products by chromatography despite several attempts.  $\text{Eu}^{3+}$  or  $\text{Gd}^{3+}$  were introduced by exchange into the bound DTPA ligands (1:1 ratio). Attempts at separating the linked and nonlinked products proved ineffective. Spectroscopic studies were therefore performed on samples containing both linked and nonlinked complexes.

Analysis of the fluorescence and phosphorescence spectra of the  $\text{Gd}^{3+}$  complexes formed with the mono- and terfluorene ligands (Figures S1–S3 in the Supporting Information) allows the identification of the energies of the singlet and triplet states for both coordinated ligands (Table 1).

Upon excitation of the F1- $\text{Eu}^{3+}$  complex, two different types of emission signals appear (Figure 2). First, a broad emission band with an apparent electronic envelope maximum at 359 nm is observed; this band is attributed to a singlet state  $^1\pi\pi^*$  transition centered on the monofluorene, as a band with similar energy was also observed in the emission spectrum of the F1- $\text{Gd}^{3+}$  complex (Figure S2 in the Supporting Information). Second, a series of sharp emission bands were observed. These bands can be attributed to transitions involving  $\text{Eu}^{3+}$  (by decreasing order of energy):  $^5\text{D}_0 \rightarrow ^7\text{F}_0$  (580 nm),  $^5\text{D}_0 \rightarrow ^7\text{F}_1$  (591 nm),  $^5\text{D}_0 \rightarrow ^7\text{F}_2$  (615 nm), and  $^5\text{D}_0 \rightarrow ^7\text{F}_4$  (696 nm).

Proof that the sensitization of  $\text{Eu}^{3+}$  is occurring through the electronic states of the monofluorene ligand is obtained by comparing the excitation spectra of F1- $\text{Eu}^{3+}$  and F1- $\text{Gd}^{3+}$  (see Figure S4 in the Supporting Information). The fact that both spectra are very similar indicates that the energy path required to induce the  $\text{Eu}^{3+}$  emission in F1- $\text{Eu}^{3+}$  is originating from the electronic structure of the chromophoric antenna F1.

The absorption spectrum of the europium terfluorene complex F3- $\text{Eu}^{3+}$  (Figure 2) exhibits two main differences

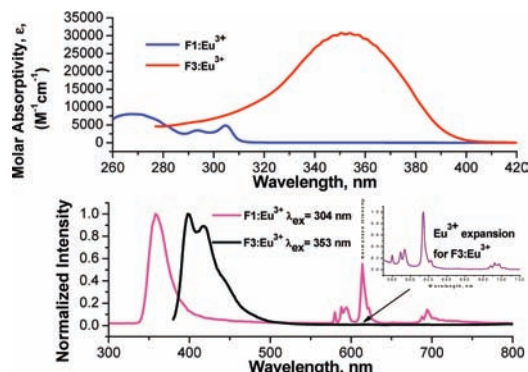
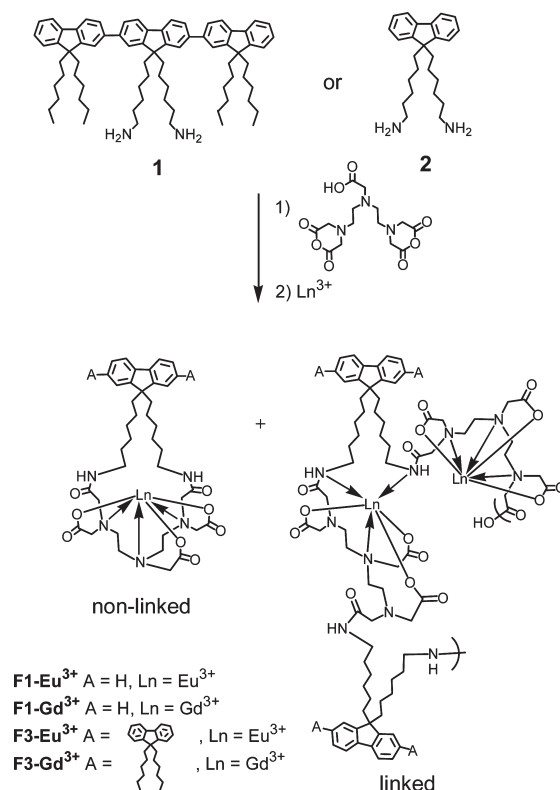


**Figure 2.** Upper: absorption spectra of both  $\text{Eu}^{3+}$  complexes formed with the mono- and terfluorene ligands in DMSO,  $80 \mu\text{M}$ , 298 K. Lower: normalized steady-state emission spectra of both  $\text{Eu}^{3+}$  complexes formed with the mono- and terfluorene ligands in DMSO,  $80 \mu\text{M}$ , 298 K. Lower inset: magnification of the  $\text{Eu}^{3+}$  signal on the spectrum of the  $\text{Eu}^{3+}$  complex formed with the terfluorene ligand in DMSO,  $80 \mu\text{M}$ , 298 K.

### Scheme 1



from that observed for F1- $\text{Eu}^{3+}$ . First, the absorption band is shifted toward significantly lower energy with an apparent maximum located at 352 nm. This shift indicates that the terfluorene group induces the lowering of the energy of the  $^1\pi\pi^*$  transition. Second, this absorption band has a significantly higher extinction coefficient relative to the monofluorene compound, which provides an advantage for practical applications: the larger absorption will induce the emission of a larger number of photons for more sensitive detection.

The emission spectrum of F3- $\text{Eu}^{3+}$  upon sensitizer excitation (Figure 2) is also significantly different from the spectrum of F1- $\text{Eu}^{3+}$  in that the overall signal emitted by this compound is dominated in intensity by a broad emission band with two apparent maxima located at 400 and 420 nm and a lower energy shoulder at approximately 445 nm.

**Table 2.** Luminescence Lifetimes of  $\text{Eu}^{3+}$  Emission and Quantum Yields upon Sensitizer Excitation in a DMSO and  $\text{CH}_2\text{Cl}_2$  Solution

| complex              |                          | luminescence lifetime (ms) <sup>a</sup> | quantum yield                           |                                |
|----------------------|--------------------------|---|---|--------------------------------|
|                      |                          |   | $\text{Eu}^{3+}$ -centered <sup>b</sup> | fluorene-centered <sup>c</sup> |
| F1– $\text{Eu}^{3+}$ | DMSO                     | 1.44 ± 0.01<br>0.51 ± 0.03              | 0.010 ± 0.002                           | 0.036 ± 0.005                  |
| F3– $\text{Eu}^{3+}$ | DMSO                     | 1.46 ± 0.01<br>0.61 ± 0.01              | 0.067 ± 0.006                           | 0.84 ± 0.08                    |
| F3– $\text{Eu}^{3+}$ | $\text{CH}_2\text{Cl}_2$ | 1.60 ± 0.02<br>0.70 ± 0.07              | 0.079 ± 0.020                           | Not recorded                   |

<sup>a</sup>  $\lambda_{\text{ex}} = 266$  nm for F1– $\text{Eu}^{3+}$ , RT; 355 nm for F3– $\text{Eu}^{3+}$ , RT. All solutions were  $10^{-3}$  M. <sup>b</sup> TbH22IAM was used as the reference.<sup>11</sup> <sup>c</sup> Quinine sulfate in 0.1 N  $\text{H}_2\text{SO}_4$  was used as the reference ( $\phi = 0.546$ ).  $\lambda_{\text{ex}} = 300$  nm for F1– $\text{Eu}^{3+}$ , and  $\lambda_{\text{ex}} = 350$  nm for F3– $\text{Eu}^{3+}$ . Concentrations of all solutions of  $\text{Eu}^{3+}$  complexes:  $7 \times 10^{-5}$  M.

The shape and wavelengths of these emission bands are similar to those observed in the fluorescence spectrum of F3– $\text{Gd}^{3+}$  (Figure S3 in the Supporting Information) and can therefore be assigned to the  $^1\pi\pi^*$  transition centered on the terfluorene moiety of the ligand bound to the lanthanide. The  $\text{Eu}^{3+}$  emission signal is also visible, although its intensity relative to the fluorene signal is smaller than that observed for F1– $\text{Eu}^{3+}$ .

The excitation spectra of the F3– $\text{Gd}^{3+}$  and F3– $\text{Eu}^{3+}$  complexes (upon monitoring of the  $^5\text{D}_0$ – $^7\text{F}_2$   $\text{Eu}^{3+}$  transition) are similar, which indicates that an  $\text{Eu}^{3+}$  energy transfer is occurring through the terfluorene electronic levels and thereby confirming that F3 is acting as a sensitizer for  $\text{Eu}^{3+}$ .

For both F1– $\text{Eu}^{3+}$  and F3– $\text{Eu}^{3+}$  complexes, the experimental luminescence decays of  $\text{Eu}^{3+}$  obtained upon ligand excitation were fitted best as the sum of two single-exponential decays (Table 2). These values can be compared to those obtained with a parent complex formed with the DTPA-derived coordinating unit: Selvin et al. have reported a unique luminescence lifetime of 0.62 ms for  $\text{Eu}^{3+}$  luminescence for a Eu–DTPA–cs124 complex.<sup>9</sup> Our results indicate the presence of two significantly different coordination environments and levels of protection against nonradiative deactivation around the lanthanide cations for both F1– $\text{Eu}^{3+}$  and F3– $\text{Eu}^{3+}$ . The two different environments present for each complex can be rationalized by the ligands F1 and F3 being a mixture of linked and nonlinked products (see the description of the synthesis). Despite the complexity of the coordination environment, it is clear that this ligand system provides equal or superior protection of the lanthanide cation against nonradiative deactivation.<sup>8</sup> The fact that the luminescence lifetimes of  $\text{Eu}^{3+}$  are similar for both F1– $\text{Eu}^{3+}$  and F3– $\text{Eu}^{3+}$  indicates that  $\text{Eu}^{3+}$  experiences similar levels of protection in both compounds and validates our building-block approach. The quantum yield values will therefore only depend on the efficiency of the energy transfer from the oligomer sensitizer to  $\text{Eu}^{3+}$ .

Quantum yields of F1– $\text{Eu}^{3+}$  and F3– $\text{Eu}^{3+}$  upon sensitizer excitation and lanthanide emission analysis have been recorded in DMSO and  $\text{CH}_2\text{Cl}_2$  (Table 2). Even if the sensitizer-to-lanthanide energy transfer is not complete, as indicated by the residual fluorescence of the fluorene moieties for each complex, values of the quantum yields for both systems are relatively high in comparison to those

reported for commercially available  $\text{Eu}^{3+}$  complexes such as  $[\text{Eu}(\text{bpy} \cdot \text{bpy} \cdot \text{bpy})^+ \text{cryptate}]^{12}$ . It is also important to note that the quantum yield of F3– $\text{Eu}^{3+}$  (in DMSO) is a 6-fold amplification of that found for F1– $\text{Eu}^{3+}$  (in DMSO), as an indication of a proportionally more efficient intramolecular energy transfer from F3 to  $\text{Eu}^{3+}$ . This finding is not readily apparent upon visual observation of the emission spectrum of F3– $\text{Eu}^{3+}$  (Figure 2) because the  $\text{Eu}^{3+}$ -centered emission appears weak when compared with the large residual of F3 terfluorene fluorescence. To evaluate the role of DMSO coordination, the lifetime and quantum yield for the F3– $\text{Eu}^{3+}$  complex in DMSO and the less coordinating solvent,  $\text{CH}_2\text{Cl}_2$ , can be compared. The relatively modest increases observed suggest that DMSO coordination is not a dominant factor.

We have demonstrated that an antenna effect for  $\text{Eu}^{3+}$  was obtained using new ligands incorporating mono- and terfluorene sensitizers. The good performance of the terfluorene sensitizer establishes that the oligomer length can be used to optimize the sensitizer-to-lanthanide energy transfer. Finally, the quantum yield of the F3– $\text{Eu}^{3+}$  complex upon  $\text{Eu}^{3+}$  monitoring can be considered as high in comparison to commercially available complexes despite the incomplete energy transfer. These results suggest that this versatile modular system has a significant potential for future applications. One of the surprising aspects of this work is that we still have a strong intensity of fluorescence arising from the fluorene unit(s), especially for the F3– $\text{Eu}^{3+}$  complex, despite a decent energy transfer to the  $\text{Eu}^{3+}$  cations, as reflected by the quantum yields. This observation indicates that the rate of intersystem crossing is not that high despite the presence of the coordinated lanthanide, which provides a heavy atom effect. For this reason, extension of this work includes rationalization of the energy migration in our system by quantifying parameters such as the efficiency of the intersystem crossing through analysis of the population of singlet and triplet states and by the recording of the luminescence lifetime.

**Acknowledgment.** This technical effort was performed in support of the National Energy Technology Laboratory's ongoing research in clean coal technology under the RDS contract DE-AC26-04NT41817. R.W.W. thanks PPG Industries for support.

**Supporting Information Available:** Emission spectra for all complexes and detailed experimental procedures. This material is available free of charge via the Internet at <http://pubs.acs.org>.

(11) Petoud, S.; Cohen, S. M.; Bünzli, J.-C. G.; Raymond, K. N. *J. Am. Chem. Soc.* **2003**, *125*, 13324–13325.

(12) Alpha, B.; Lehn, J.-M.; Mathis, G. *Angew. Chem., Int. Ed.* **1987**, *26*, 266–267. Alpha, B.; Balzani, V.; Lehn, J.-M.; Perathoner, S.; Sabbatini, N. *Angew. Chem., Int. Ed.* **1987**, *26*, 1266–1267.